Ion flux characteristics in high-power pulsed magnetron sputtering discharges

A Letters Journal Exploring the Frontiers of Physics

February 2007

EPL, **77** (2007) 45002
doi: 10.1209/0295-5075/77/45002

www.epljournal.org

Ion flux characteristics in high-power pulsed magnetron sputtering discharges

J. Vlček, P. Kudláček, K. Burcalová and J. Musil

Department of Physics, University of West Bohemia - Univerzitní 22, 30614 Plzeň, Czech Republic

received 22 September 2006; accepted in final form 12 December 2006
published online 2 February 2007

PACS 52.50.Dg – Plasma sources
PACS 52.70.-m – Plasma diagnostic techniques and instrumentation
PACS 52.77.-j – Plasma applications

Abstract – High-power pulsed dc magnetron discharges for ionized high-rate sputtering of copper films were investigated. The repetition frequency was 1 kHz at a fixed 20% duty cycle and argon pressures of 0.5 Pa and 5 Pa. Time evolutions of the discharge characteristics were measured at a target power density in a pulse up to 950 W/cm^2. Time-averaged mass spectroscopy was performed at substrate positions. It was shown that copper ions are strongly dominant (up to 92%) in total ion fluxes onto the substrate. Their energy distributions with a broadened low-energy part at a lower pressure are extended to higher energies (up to 45 eV relative to ground potential for the target-to-substrate distance of 100 mm).

Introduction. – Recently, novel high-power pulsed dc magnetron systems have been used for sputtering of films [1–6]. The target power loading in a pulse of these discharges with a peak value up to several kW/cm^2 is considerably higher than a typical maximum target power loading (usually less than 20 W/cm^2) applied in conventional dc magnetron sputtering. Consequently, film deposition can be carried out at highly ionized fluxes of sputtered atoms. This is of great interest for directional deposition into high aspect ratio trench and via structures, and for ion-assisted growth of films. Fundamental aspects of the high-power pulsed magnetron sputtering and its new technological applications were discussed in refs. [7–9].

The energy distribution of individual ions bombarding the growing films and composition of total ion fluxes onto a substrate are of key importance for characterization of these high-power pulsed sputter sources and for a good understanding of the complicated deposition processes. However, only the results obtained using an energy-resolved mass spectrometer in a position parallel to the target surface and outside the substrate region are available so far [4,10]. The main reason are very large fluxes of highly ionized sputtered atoms at high target power loadings in pulses. In this work, we report on time-averaged mass spectroscopy performed at a substrate location to investigate ion energy distributions and composition of total ion fluxes onto the substrate during high-power pulsed magnetron sputtering of a copper target in argon gas under various discharge conditions. The spectrometer was placed at the target-substrate axis in a position directly facing the target surface. The main aim of this letter was to show fundamental changes in the ion flux characteristics in these high-power pulsed discharges compared with conventional dc magnetron sputtering discharges. Moreover, the effects of the gas pressure and the target-to-substrate distance on the ion flux characteristics were investigated at high values of the average pulse target power density.

Experimental details. – The experiments were performed using a strongly unbalanced magnetron source with a directly water-cooled planar copper target (diameter 100 mm and thickness 8 mm) in a standard stainless-steel vacuum chamber (diameter 507 mm and length 520 mm), which was evacuated by a diffusion pump (2000 l/s) backed up with a rotary pump (30 m^3/h). The maximum parallel component of the magnetic induction above the racetrack region, measured at the distance $z = 4$ mm from the target surface, was 320 G. The absolute values of the corresponding vertical component, being up to 1360 G at the target surface, were approximately 30 G and 10 G for $z = 60$ mm and 180 mm, respectively. The magnetron was driven by a pulsed dc power supply (Rübig MP120) working in the frequency range from 0.5 kHz to 50 kHz with a maximum voltage and current of 1 kV and 120 A, respectively. In the present work, the

argon pressure, p, was 0.5 Pa and 5 Pa at the repetition frequency $f_r = 1$ kHz and the voltage pulse duration $t_1 = 200\,\mu$s, *i.e.*, at a fixed duty cycle $t_1/T = 20\%$, where the pulse period $T = 1/f_r$. This value is sufficiently low to avoid overheating of the target and any discharge instabilities at high target power loadings, but it is sufficiently high to achieve very high deposition rates of films. The target-to-substrate distance, d, was 100 mm and 200 mm.

Waveforms of the magnetron voltage, $U_d(t)$, and the discharge current, $I_d(t)$, were recorded using our own software, which was also applied to evaluate the respective average pulse current, I_{da}. This was carried out by a computer controlling the operation of the power supply with the use of the formula

$$I_{da} = \frac{1}{t_1}\int_0^{t_1} I_d(t)\mathrm{d}t. \qquad (1)$$

The same integral expression was used for calculation of the average pulse voltage, U_{da}. The substrate current, $I_s(t)$, was measured using a flat circular probe with a diameter of 10 mm, located in the center of the substrate holder and electrically isolated from it. The negative probe bias remained constant at $U_b = -50$ V during the pulse to repel high-energy electrons produced. Waveforms of the $I_s(t)$ currents were monitored by a digital ETC M621 Oscilloscope using a Tektronix P6042 Current probe (dc to 50 MHz).

The energy distribution of positive ions incident upon a central region of the substrate was measured with an energy-resolved mass spectrometer (EQP 300 Hiden Analytical) placed at the target-substrate axis in a position directly facing the target surface. To perform these measurements under conditions of very large fluxes of highly ionized sputtered atoms at high target power loadings during pulses, a grounded cylindrical shielding shutter with a 10 mm diameter hole in the center was located 5 mm in front of a special end cap of the mass spectrometer barrel. The diameter (160 mm) of the shielding shutter was the same as that of the substrate holder. We used a modified configuration of the cap in which an extraction electrode with a 50 μm diameter orifice in the center was placed 2.5 mm behind a grounded front electrode of the spectrometer with a central input aperture of 1 mm in diameter. In the present work, the ion energy distributions were obtained for 350 individual values of the ion energy. For each ion energy the data were measured 30 times and then averaged. Two isotopes of copper (^{63}Cu and ^{65}Cu) and argon (^{36}Ar and ^{40}Ar) were considered. Owing to the same behaviour of the different isotopes, sums of the corresponding isotope contributions were presented. The integral fluxes of individual ionic species were determined by a direct integration of the respective time-averaged energy distributions. Their calibration was carried out using the corresponding average substrate ion current density, $\bar{J}_{is}$, calculated over a whole pulse period, T, from the measured $I_s(t)$ values after subtracting the secondary electrons component [11]. The average energy of individual ions arriving at the substrate, $\bar{E}_{is}$, was determined by a standard integral formula using the corresponding ion energy distributions.

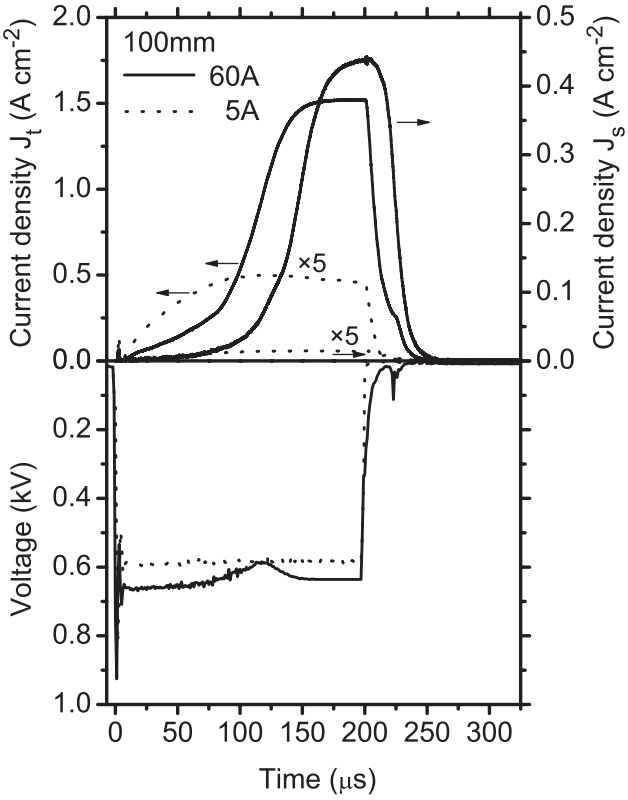

Fig. 1: Waveforms of the magnetron voltage, U_d, the target current density, J_t, and the substrate current density, J_s, for preset average pulse currents $I_{da} = 60$ A (full curves) and $I_{da} = 5$ A (dotted curves, see 5 times magnified J_t and J_s values) at a pressure $p = 0.5$ Pa and a substrate distance $d = 100$ mm.

Results. – Figures 1 and 2 show time evolutions of the magnetron voltage, $U_d(t)$, the target current density $J_t(t) = I_d(t)/A_t$, where A_t is a total area of the target (78.5 cm^2 in our case), and the substrate current density, $J_s(t)$, during pulses at the average pulse currents $I_{da} = 5$ A and 60 A. They provide information on absorption of energy in the discharge plasma at the pressures $p = 0.5$ Pa and 5 Pa, and on transfer of arising ions to the substrate at the distances $d = 100$ mm and 200 mm.

As is shown in fig. 1, the maximum target power loading in a pulse was 950 W/cm^2 at $I_{da} = 60$ A and $p = 0.5$ Pa with the corresponding maximum target current density $J_t = 1.5$ A/cm^2 and maximum substrate current density $J_s = 0.44$ A/cm^2 for the substrate distance $d = 100$ mm. The average pulse target power density $S_{da} = U_{da}J_{da}$, where $J_{da} = I_{da}/A_t$, was 480 W/cm^2 and the average target power density over a pulse period $\bar{S}_d = S_{da}t_1/T$ was 96 W/cm^2 under these conditions. For comparison,

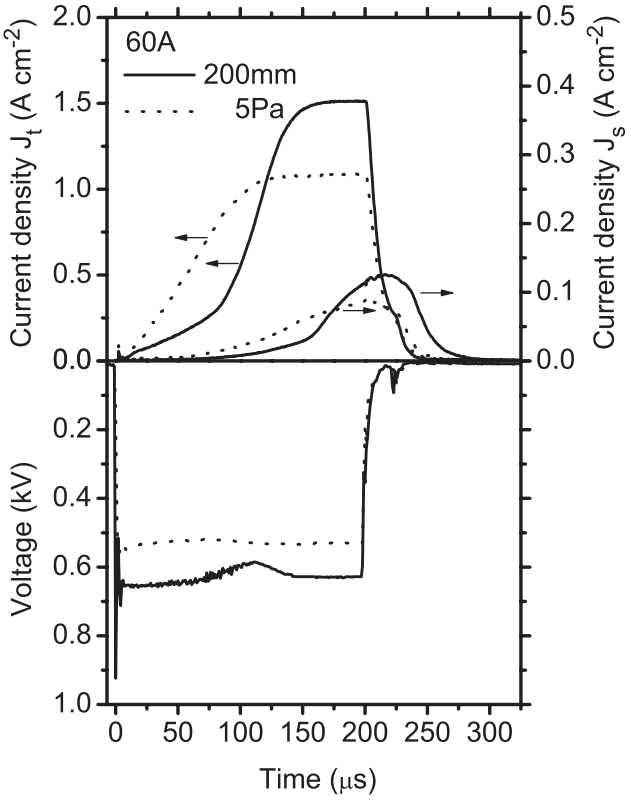

Fig. 2: Waveforms of the magnetron voltage, U_d, the target current density, J_t, and the substrate current density, J_s, for a preset average pulse current $I_{da} = 60\,\mathrm{A}$ at a pressure $p = 0.5\,\mathrm{Pa}$ and a substrate distance $d = 200\,\mathrm{mm}$ (full curves) or $p = 5\,\mathrm{Pa}$ and $d = 100\,\mathrm{mm}$ (dotted curves).

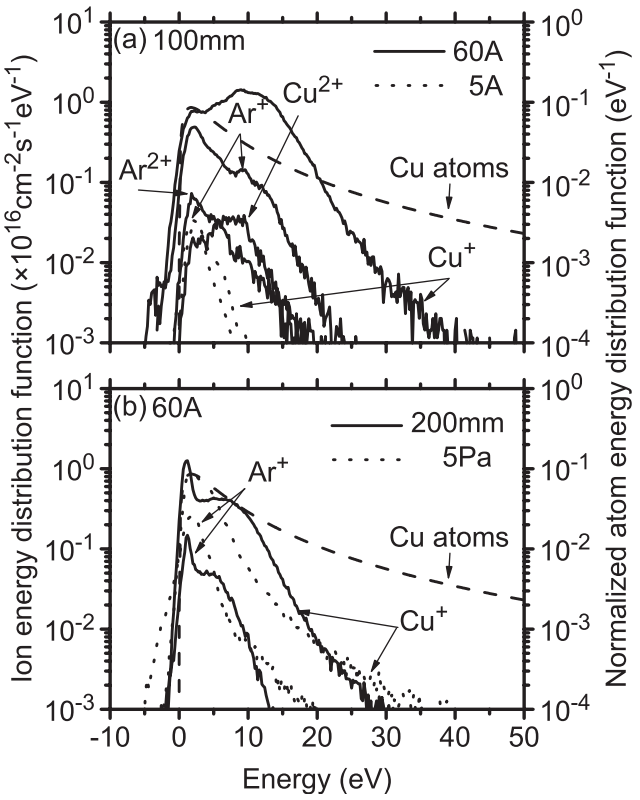

Fig. 3: Time-averaged energy distributions of copper and argon ions at substrate positions for preset average pulse currents $I_{da} = 5\,\mathrm{A}$ and $60\,\mathrm{A}$ at a pressure $p = 0.5\,\mathrm{Pa}$ and a substrate distance $d = 100\,\mathrm{mm}$ (a), and for $I_{da} = 60\,\mathrm{A}$ at $p = 0.5\,\mathrm{Pa}$ and $d = 200\,\mathrm{mm}$ or $p = 5\,\mathrm{Pa}$ and $d = 100\,\mathrm{mm}$ (b). For comparison, a normalized energy distribution of sputtered Cu atoms at the target surface (calculated using eq. (2)) is presented.

the waveforms obtained at $I_{da} = 5\,\mathrm{A}$ and $p = 0.5\,\mathrm{Pa}$, when the average pulse target power density $S_{da} = 37\,\mathrm{W/cm^2}$ and the average target power density over a pulse period $\bar{S}_d = 7.4\,\mathrm{W/cm^2}$, are presented in fig. 1. The aim was to show an experimental situation relatively close to that in conventional dc magnetron sputtering discharges.

As can be seen in fig. 2, the enhanced value of the pressure $p = 5\,\mathrm{Pa}$ leads to a decrease of the average pulse voltage, keeping a constant value of $I_{da} = 60\,\mathrm{A}$, from $U_{da} = 630\,\mathrm{V}$ obtained for $p = 0.5\,\mathrm{Pa}$ (see fig. 1) to $U_{da} = 525\,\mathrm{V}$. As a result, the corresponding value of the average pulse target power density decreased from $480\,\mathrm{W/cm^2}$ to $400\,\mathrm{W/cm^2}$. The related average target power density over a pulse period, $\bar{S}_d$, was reduced from $96\,\mathrm{W/cm^2}$ to $80\,\mathrm{W/cm^2}$. The average substrate ion current density, $\bar{J}_{is}$, decreased 3.8 times for $p = 5\,\mathrm{Pa}$ and $d = 100\,\mathrm{mm}$. This can be mainly explained by a stronger decrease of the electron impact ionization efficiency in a plasma bulk with the distance from the target, particularly at the lower applied target power density leading to a reduced number of sputtered copper atoms. Let us note that the ionization energy of copper (7.72 eV) is significantly lower compared with both the ionization limits of argon (15.76 eV and 15.94 eV). Moreover, enhanced losses of the ions due to their scattering on argon atoms during transport to the substrate must be considered at 5 Pa. Owing to the higher ion losses to chamber walls during transport to the substrate at the distance of 200 mm from the target, the $\bar{J}_{is}$ value decreased 3.3 times compared with $d = 100\,\mathrm{mm}$ (fig. 1) at the same values of $I_{da} = 60\,\mathrm{A}$ and $p = 0.5\,\mathrm{Pa}$. The increase in the substrate distance from $d = 100\,\mathrm{mm}$ to 200 mm resulted in only negligible differences between the corresponding $U_d(t)$ and $J_t(t)$ time evolutions (see figs. 1 and 2).

Figure 3 shows the time-averaged energy distributions of copper and argon ions measured at a center of the substrate. For the basic set of the deposition parameters ($I_{da} = 60\,\mathrm{A}$, $p = 0.5\,\mathrm{Pa}$ and $d = 100\,\mathrm{mm}$), the energy distributions of all the detected ions, including Cu^{2+} and Ar^{2+}, are given (fig. 3a). In the other cases, only the results obtained for the most populated Cu^+ and Ar^+ ions are shown. As is seen in fig. 3, the Cu^+ ions become strongly dominant in a total ion flux onto the substrate at high values of the target power loading (see $I_{da} = 60\,\mathrm{A}$). Under these conditions, their energy distributions are extended to higher energies (up to 45 eV relative to ground potential) compared with those for the Ar^+ ions. The Cu^+ ion energy distribution originates mainly

Table 1: The average energy of Cu^+ and Ar^+ ions, $\bar{E}_{is}$, and composition of total ion fluxes at two substrate positions ($d = 100$ mm and 200 mm) for preset average pulse currents $I_{da} = 5$ A and 60 A, and two pressures ($p = 0.5$ Pa and 5 Pa).

Deposition parameters			$\bar{E}_{is}$ (eV)		Composition of total ion flux (%)			
I_{da} (A)	p (Pa)	d (mm)	Cu^+	Ar^+	Cu^+	Cu^{2+}	Ar^+	Ar^{2+}
5	0.5	100	3.8	2.7	47.7	0.3	46.8	5.2
60	0.5	100	9.3	5.3	82.5	1.5	14.3	1.7
60	0.5	200	5.2	3.6	90.2	1.4	7.8	0.6
60	5.0	100	4.2	2.7	79.9	0.1	18.7	1.3

from the kinetic energy distribution of sputtered Cu atoms at the target [12–14]. The ions are then formed predominantly by electron impact ionization at a time-dependent plasma potential near the target and in a plasma bulk. However, also Cu^+ ion-produced neutrals reflected from the target might be important due to a high degree of redirection of the ionized sputtered Cu atoms back to the target in these high-power sputter sources [8]. The kinetic energy of the emitted atoms is described by Thompson's theory of atomic collision cascades [15] for incoming ions of moderate energy (hundreds of eV). The normalized cascade distribution is [16]

$$F(E) = \begin{cases} 2\left(1 + \dfrac{E_b}{\Lambda E_{it}}\right)^2 \dfrac{E_b E}{(E_b + E)^3}, & \text{for} \quad E \leqslant \Lambda E_{it}, \\ 0, \quad \text{for} \quad E > \Lambda E_{it}. \end{cases} \tag{2}$$

Here, E is the kinetic energy of the sputtered atom, E_{it} is the energy of ions incident on the target, E_b is the surface binding energy of the target material ($E_b = 3.49$ eV for Cu), ΛE_{it} is the maximum recoil energy, and $\Lambda = 4M_iM_a/(M_i + M_a)^2$, where M_i and M_a are the masses of the incident ions and the sputtered atoms, respectively. Part of the normalized distribution of initial energies for Cu atoms being sputtered by Ar^+ ions at 600 eV (see the U_{da} values in figs. 1 and 2) is shown in fig. 3. Let us note that the calculated values of the distribution function $F(E)$ in fig. 3 are practically the same also for sputtering of the Cu target by Cu^+ ions (so-called self-sputtering). The self-sputtering of the copper target is typical for high-power pulsed magnetron sputter sources due to a high self-sputtering yield of copper and high degree of ionization of sputtered atoms near the target [8]. A low-energy peak of the Ar^+ ion distributions corresponds to slow Ar atoms ionized at a low plasma potential. The higher-energy part of these distributions can be attributed either to the Ar atoms which gain energy in collisions with the sputtered Cu atoms [12] or to Ar^+ ion-produced neutrals reflected from the target [13]. To understand a shift of the maximum of the Cu^+ ion distribution to a higher energy compared with that of the Ar^+ ion distribution at $I_{da} = 60$ A, $p = 0.5$ Pa and $d = 100$ mm (fig. 3a), it should be taken into account that plasma potential increases during a pulse (see Langmuir probe measurements in ref. [17]) and that most of the Cu^+ ions are formed in a later stage of these high-power pulses when argon gas is strongly rarefied [4]. As expected, the ion energy distributions become narrower (fig. 3b) and the corresponding average energies of ions, $\bar{E}_{is}$, decrease (table 1) with a rise in the pressure and the substrate distance. This is caused by a combined effect of the energy transfer from sputtered Cu atoms to Ar gas atoms and from Cu^+ and Ar^+ ions to the Ar atoms with the aforementioned scattering of these ions during transport to the substrate. Moreover, the changes in the discharge characteristics at a higher pressure must be considered (fig. 2).

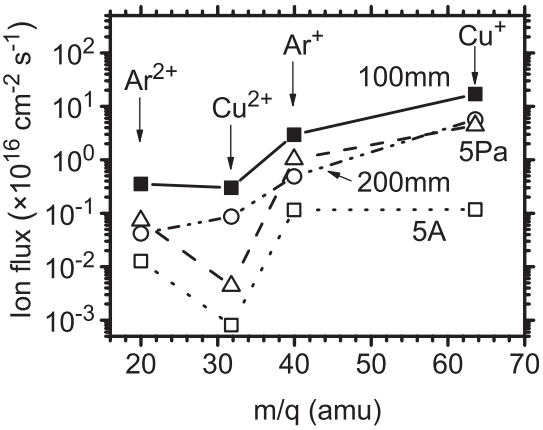

Fig. 4: Integral ion fluxes of copper and argon ions for a preset average pulse current $I_{da} = 60$ A at a pressure $p = 0.5$ Pa and substrate distances $d = 100$ mm (full curve) and $d = 200$ mm (chain curve), for $I_{da} = 60$ A at $p = 5$ Pa and $d = 100$ mm (dashed curve), and for $I_{da} = 5$ A at $p = 0.5$ Pa and $d = 100$ mm (dotted curve).

Composition of the total ion fluxes onto the substrate and the absolute values of individual ion fluxes are given in table 1 and fig. 4, respectively. As is shown in table 1, an increase in the I_{da} values from 5 A to 60 A at $p = 0.5$ Pa and $d = 100$ mm results in an enlarged total fraction of Cu^+ and Cu^{2+} ions in the ion flux onto the substrate from 48% (at 0.3% of the Cu^{2+} ions) to 84% (at 1.5% of the Cu^{2+} ions), respectively. The corresponding value of the average substrate ion current density, $\bar{J}_{is}$, increased 82 times at $I_{da} = 60$ A (see figs. 1 and 4). Almost 92% fraction

of copper ions in the total ion flux onto the substrate at $I_{da} = 60\,\mathrm{A}$, $p = 0.5\,\mathrm{Pa}$ and $d = 200\,\mathrm{mm}$ can be explained by a weaker ionization of Ar atoms compared with Cu atoms at the distances $z > 100\,\mathrm{mm}$ from the target in the investigated plasma with enhanced magnetic confinement. As can be seen in table 1, the increase in the pressure from 0.5 Pa to 5 Pa at $I_{da} = 60\,\mathrm{A}$ and $d = 100\,\mathrm{mm}$ leads to relatively small changes in the fractions of argon ions (from 16% to 20%, respectively) and copper ions (from 84% to 80%, respectively) in the total ion flux. This is caused by a stronger rarefaction of the argon gas during pulses at $p = 5\,\mathrm{Pa}$ and by the weaker ionization of Ar atoms in a plasma bulk due to lower electron temperatures at the higher pressure.

Conclusion. – It was shown that copper ions are strongly dominant (up to 92%) in total ion fluxes onto the substrate at high target power densities (up to $950\,\mathrm{W/cm^2}$ in a pulse) in pulsed magnetron sputtering discharges. Their energy distributions are extended to higher energies (up to 45 eV relative to ground potential) compared with those for the Ar^+ ions (up to 25 eV). The Cu^+ ion energy distribution originates mainly from the kinetic energy distribution of sputtered Cu atoms at the target. Very effective sputtering and ionization of copper atoms in a later stage of high-power pulses, when the plasma potential is increased, results in a broadened low-energy part (up to 15 eV) of the Cu^+ ion distribution at a lower pressure. Moreover, also Cu^+ ion-produced neutrals reflected from the target might be important due to a high degree of redirection of the ionized sputtered Cu atoms back to the target in these high-power sputtering discharges.

* * *

This work was supported by the Ministry of Education of the Czech Republic under Project No. MSM 4977751302.

REFERENCES

[1] Kouznetsov V., Macák K., Schneider J. M., Helmersson U. and Petrov I., *Surf. Coat. Technol.*, **122** (1999) 290.
[2] Macák K., Kouznetsov V., Schneider J., Helmersson U. and Petrov I., *J. Vacuum Sci. Technol. A*, **18** (2000) 1533.
[3] Ehiasarian A. P., Hovsepian P. Eh., Hultman L. and Helmersson U., *Thin Solid Films*, **457** (2004) 270.
[4] Vlček J., Pajdarová A. D. and Musil J., *Contrib. Plasma Phys.*, **44** (2004) 426.
[5] Vašina P., Meško M., Ganciu M., Bretagne J., Boisse-Laporte C., de Poucques L. and Touzeau M., *Europhys. Lett.*, **72** (2005) 390.
[6] Konstantinidis S., Dauchot J. P., Ganciu M., Ricard A. and Hecq M., *J. Appl. Phys.*, **99** (2006) 013307.
[7] Anders A., *Surf. Coat. Technol.*, **183** (2004) 301.
[8] Christie D. J., *J. Vacuum Sci. Technol. A*, **23** (2005) 330.
[9] Helmersson U., Lattemann M., Bohlmark J., Ehiasarian A. P. and Gudmundsson J. T., *Thin Solid Films*, **513** (2006) 1.
[10] Bohlmark J., Ehiasarian A. P., Lattemann M., Alami J. and Helmersson U., *Society of Vacuum Coaters 505/856-7188, 48th Annual Technical Conference Proceedings* (2005) ISSN 0737-5921, p. 470.
[11] Lieberman M. A. and Lichtenberg A. J., *Principles of Plasma Discharges and Materials Processing* (Wiley-Interscience, New York) 1994, p. 282.
[12] Kadlec S., Quaeyhaegens C., Knuyt G. and Stals L. M., *Surf. Coat. Technol.*, **89** (1997) 177.
[13] Mišina M., Shaginyan L. R., Maček M. and Panjan P., *Surf. Coat. Technol.*, **142-144** (2001) 348.
[14] Bradley J. W., Bäcker H., Aranda-Gonzalvo Y., Kelly P. J. and Arnell R. D., *Plasma Sources Sci. Technol.*, **11** (2002) 165.
[15] Thompson M. W., *Philos. Mag.*, **18** (1968) 377.
[16] Lu J. and Kushner M. J., *J. Appl. Phys.*, **87** (2000) 7198.
[17] Pajdarová A. D., PhD Thesis, University of West Bohemia, Plzeň, Czech Republic (2005).